

A Case Study of Urban Particle Acidity and Its Influence on Secondary Organic Aerosol

QI ZHANG,^{*,†} JOSE L. JIMENEZ,[‡]
DOUGLAS R. WORSNOP,[§] AND
MANJULA CANAGARATNA[§]

Atmospheric Sciences Research Center (ASRC) and Department of Environmental Health Sciences, 251 Fuller Road, CESTM L110, University at Albany, State University of New York, Albany, New York 12203, Cooperative Institute for Research in Environmental Sciences (CIRES) and Department of Chemistry and Biochemistry, 216 UCB, University of Colorado-Boulder, Boulder, Colorado 80309, and Aerodyne Research Inc., Billerica, Massachusetts 01821

Size-resolved indicators of aerosol acidity, including H^+ ion concentrations (H^+_{Aer}) and the ratio of stoichiometric neutralization are evaluated in submicrometer aerosols using highly time-resolved aerosol mass spectrometer (AMS) data from Pittsburgh. The pH and ionic strength within the aqueous particle phase are also estimated using the Aerosol Inorganics Model (AIM). Different mechanisms that contribute to the presence of acidic particles in Pittsburgh are discussed. The largest H^+_{Aer} loadings and lowest levels of stoichiometric neutralization were detected when PM_{10} loadings were high and dominated by SO_4^{2-} . The average size distribution of H^+_{Aer} loading shows an accumulation mode at $D_{va} \approx 600$ nm and an enhanced smaller mode that centers at $D_{va} \approx 200$ nm and tails into smaller sizes. The acidity in the accumulation mode particles suggests that there is generally not enough gas-phase NH_3 available on a regional scale to completely neutralize sulfate in Pittsburgh. The lack of stoichiometric neutralization in the 200 nm mode particles is likely caused by the relatively slow mixing of gas-phase NH_3 into SO_2 -rich plumes containing younger particles. We examined the influence of particle acidity on secondary organic aerosol (SOA) formation by comparing the mass concentrations and size distributions of oxygenated organic aerosol (OOA—surrogate for SOA in Pittsburgh) during periods when particles are, on average, acidic to those when particles are bulk neutralized. The average mass concentration of OOA during the acidic periods ($3.1 \pm 1.7 \mu g m^{-3}$) is higher than that during the neutralized periods ($2.5 \pm 1.3 \mu g m^{-3}$). Possible reasons for this enhancement include increased condensation of SOA species, acid-catalyzed SOA formation, and/or differences in air mass transport and history. However, even if the entire enhancement ($\sim 0.6 \mu g m^{-3}$) can be attributed to acid catalysis, the upper-bound increase of SOA mass in acidic particles is $\sim 25\%$, an enhancement that is much more moderate than the multifold increases in SOA mass observed during some lab

studies and inferred in SO_2 -rich industrial plumes. In addition, the mass spectra of OOA from these two periods are almost identical with no discernible increase in relative signal intensity at larger m/z 's (> 200 amu), suggesting that the chemical nature of SOA is similar during acidic and neutralized periods and that there is no significant enhancement of SOA oligomer formation during acidic particle periods in Pittsburgh.

1. Introduction

Acidic aerosols are ubiquitous in the atmosphere with significant implications for human health (1) and ecological integrity (2). Atmospheric acidic aerosols tend to be more hygroscopic than their neutralized form, as indicated by the positive correlations between particle phase acidity and measured water content (3) and between deliquescence RH of ambient particles and their NH_4^+/SO_4^{2-} ratio (4). Larger hygroscopicity enhances particles' ability to scatter light and to nucleate cloud droplets, and thus their influence on visibility and climate.

Particle phase acidity has also been linked to secondary aerosol formation. Acid-catalyzed heterogeneous reactions, for instance, have been proposed as an important mechanism that might significantly enhance secondary organic aerosol (SOA) production in the atmosphere (5–8). Up to several-fold increases in SOA mass have been observed in chamber studies when acidic seed particles were used (e.g., refs 5, 6). Similar multifold enhancements in SOA production in the Houston area could be inferred based on the particle volume growth rates measured in industrial plumes rich in SO_2 and volatile organic compounds (VOCs) compared to those containing only VOCs or SO_2 (9). In addition, Chu (10) observed simultaneous increases of OC and SO_4^{2-} mass concentrations accompanied with a charge deficit of NH_4^+ during regional high $PM_{2.5}$ episodes in the Eastern U.S. and thus suggested a link between acidic particles and summertime SOA formation. However, while analyzing the aerosol mass spectrometer (AMS) data from Pittsburgh, we observed no statistically significant enhancement in the total organic mass concentration in acidic particles compared to the bulk neutralized particles (11). Similarly, Takahama et al. (12) evaluated the correlations between OC/EC ratio and particle acidity using semi-continuous data from the Pittsburgh Air Quality Study (PAQS) and concluded that acid-catalyzed SOA is not large enough to be observed consistently above their analytical uncertainties and particle concentration variations due to transport and mixing.

The chemistry and effects of acidic aerosols are intimately linked to a variation of acidity as a function of particle size. We thus investigate size-resolved indicators of ambient aerosol acidity using an AMS in Pittsburgh and exploit the high time resolution of these measurements (5–10 min) to resolve different mechanisms that contribute to the presence of acidic particles. Particle acidity is evaluated based on the ion balance between NH_4^+ and the inorganic anions (SO_4^{2-} , NO_3^- , and Cl^-), an approach that is commonly taken (e.g., refs 4, 13, 14–18) and is applicable for this study because submicrometer particles in Pittsburgh generally contain very low levels of metal ions (e.g., Na^+ , Ca^{2+} , and K^+) (19, 20). We also use the chemical speciation data from the AMS as inputs to the Aerosol Inorganic Model (21) to estimate the ionic strength and pH of the particles.

Compared to previous work on ambient aerosol acidity that utilized filter measurements (e.g., refs 4, 18), the high

* Corresponding author phone: (518) 437-8752; fax: (518) 437-8758; e-mail: qz@asrc.cestm.albany.edu.

[†] University at Albany, State University of New York.

[‡] University of Colorado-Boulder.

[§] Aerodyne Research Inc.

time resolution of AMS data enables us to avoid the various problems associated with the low time resolution of filter sampling (13) and, additionally, to examine the sources and effects of acidity on particle characteristics such as the size distribution, and the potential influence of aerosol acidity on the ambient SOA concentration. We also build on previous work which has shown that AMS organic aerosol mass spectra can be deconvolved to determine oxygenated and hydrocarbon-like organic aerosol (OOA and HOA) components (22) and that in Pittsburgh (23) (as well as during some periods in Mexico City (24)), OOA is mostly SOA, and HOA is mostly primary OA (POA) associated with fossil fuel combustion. The ability to directly correlate measures of particle acidity with the mass of OOA (a surrogate for SOA) rather than total organic aerosol mass (POA + SOA) or OC/EC ratios, which has been done in the few ambient studies that have examined this issue in the past (10–12), is a new and unique component of our analysis.

2. Experimental Methods

A Quadrupole-AMS was deployed at the Pittsburgh EPA Supersite from September 7 to 22, 2002. The mass concentrations and size distributions of nonrefractory (NR) chemical species (e.g., SO_4^{2-} , NO_3^- , NH_4^+ , Cl^- , and organics) were determined in submicrometer particles (approximately PM_{10}) and used for the analysis in this study. Overviews on the sampling site, local meteorology, AMS operation, and general data analysis are given in previous publications (11, 20). Details on the organic mass spectral analysis and discussions on HOA and OOA are presented in Zhang et al. (22, 23). Presented here is only information pertinent to this study. A particle collection efficiency (CE) correction was applied to account for particle bounce in the AMS vaporizer (11). Although some studies have observed higher CE values in the AMS for acidic sulfate-containing particles (25), this effect is only observed for particles much more acidic than those in this study, and thus does not affect the quantification of species during the acidic and neutralized periods presented here.

3. Indicators of Acidity

3.1. H^+_{Aer} . The mass and molar concentrations (in ng m^{-3} and nmol m^{-3} , respectively) of H^+ present in the particle-phase per unit volume of air, H^+_{Aer} , are directly estimated from AMS measurements as the difference between the NH_4^+ mass concentrations measured in the particles and the stoichiometric NH_4^+ concentrations required to fully neutralize the measured concentrations of SO_4^{2-} , NO_3^- , and Cl^- :

$$\text{H}^+_{\text{Aer}} = 2 \times \text{SO}_4^{2-}/96 + \text{NO}_3^-/62 + \text{Cl}^-/35.5 - \text{NH}_4^+/18 \quad (1)$$

where, NH_4^+ , SO_4^{2-} , NO_3^- , and Cl^- denote the mass concentrations (in ng m^{-3}) of the species and the denominators correspond to their molecular weights. Other ionic species, such as NaCl , are not included in eq 1 because they do not have a large contribution to the observed $\text{PM}_{2.5}$ mass, e.g., the average mole-equivalent concentration of metal ions in $\text{PM}_{2.5}$ is only ~6–7% of that of NH_4^+ in Pittsburgh (calculated from ref 19). More importantly, most chemical forms of these species do not vaporize at the AMS temperature of 600 °C, so their perturbation of the anion/cation balance calculated here will be even smaller.

3.2. $\text{NH}_4^+_{\text{meas}}/\text{NH}_4^+_{\text{neu}}$. The degree of stoichiometric neutralization for the ensemble of measured particles is obtained from the normalized ratio of the measured NH_4^+ concentration (in nmol m^{-3}) to the NH_4^+ concentration needed for full neutralization of the anions,

$$\text{NH}_4^+_{\text{meas}}/\text{NH}_4^+_{\text{neu}} = \text{NH}_4^+/18 / (2 \times \text{SO}_4^{2-}/96 + \text{NO}_3^-/62 + \text{Cl}^-/35.5) \quad (2)$$

In this manuscript, we use the $\text{NH}_4^+_{\text{meas}}/\text{NH}_4^+_{\text{neu}}$ ratio to identify “neutralized particle periods” ($\text{NH}_4^+_{\text{meas}}/\text{NH}_4^+_{\text{neu}} = 1 \pm \sigma$) and “more acidic particle periods” ($\text{NH}_4^+_{\text{meas}}/\text{NH}_4^+_{\text{neu}} < 0.75 + 1\sigma$), where σ is the corresponding analytical error for $\text{NH}_4^+_{\text{meas}}/\text{NH}_4^+_{\text{neu}}$ calculated for every datapoint in time based on error propagation of the measurement uncertainty and noise for NH_4^+ , SO_4^{2-} , Cl^- , and NO_3^- . On average, σ is 4% of the corresponding $\text{NH}_4^+_{\text{meas}}/\text{NH}_4^+_{\text{neu}}$ value. Since concentrations of NO_3^- and Cl^- in acidic particles are usually very small, $\text{NH}_4^+_{\text{meas}}/\text{NH}_4^+_{\text{neu}} \approx 0.75$ indicates roughly equal mole concentrations of $(\text{NH}_4)_2\text{SO}_4$ and NH_4HSO_4 . In total, the “more acidic” and “neutralized” periods account for ~30 and 25%, respectively, of the total sampling time of this study. The rest of the data points fall into a mildly acidic regime and are not analyzed separately.

3.3. pH. The pH, which is related to the concentration of H^+ within the aqueous environment (H^+_{aq}) of the ambient particles, is the acidity measure that most likely influences the chemical behavior of aerosol particles. Since the AMS does not directly measure H^+_{aq} , we use the H^+_{Aer} calculated from AMS measurements to estimate the pH and ionic strength within the aqueous particle phase using the on-line Aerosol Inorganics Model (AIM, Model II) (<http://www.hpc1.uea.ac.uk/~e770/aim.html>). Inputs to the model include the molar concentrations of sulfate, nitrate, ammonium and H^+_{Aer} (nmol m^{-3}), ambient temperature, and relative humidity (RH). Details on the model are given in Clegg et al. (21). Note that this model neglects the influence of organics on water uptake and on the partitioning of the inorganic species. While organics can lead to modest increases of water uptake (26), this increase is expected have a minor effect on partitioning/dissociation of inorganic species in acidic particles. Based on model outputs, we calculated the pH and the ionic strength (I) in aerosols:

$$\text{pH} = -\log(\text{fH}^+_{\text{aq}} \times \text{xH}^+_{\text{aq}}) \quad (3)$$

$$I = 1/2 (\text{mH}^+_{\text{aq}} + \text{mHSO}_4^-_{\text{aq}} + \text{mSO}_4^{2-}_{\text{aq}} \times 4 + \text{mNO}_3^-_{\text{aq}} + \text{mNH}_4^+_{\text{aq}}) \quad (4)$$

fH^+_{aq} and xH^+_{aq} are the activity coefficient on mole fraction basis and the mole fractions of aqueous particle phase H^+ , respectively. $\text{fH}^+_{\text{aq}} \times \text{xH}^+_{\text{aq}}$ represents the aqueous phase activity of H^+ . mH^+_{aq} , $\text{mHSO}_4^-_{\text{aq}}$, $\text{mSO}_4^{2-}_{\text{aq}}$, $\text{mNO}_3^-_{\text{aq}}$, and $\text{mNH}_4^+_{\text{aq}}$ are the molalities (in mol/kg of water) of each species.

Note that these calculations depend on the presence of an aqueous phase in thermodynamic equilibrium. Metastable aerosols are not evaluated in this study. Thus, if the ambient RH is less than the deliquescence RH of the predominant solid phase (i.e., ~30% for NH_4HSO_4 and ~80% for $(\text{NH}_4)_2\text{SO}_4$), the pH and ionic strength are not estimated. The output of the model is not reported for periods with $\text{H}^+_{\text{Aer}} \leq 0$ ($\text{NH}_4^+_{\text{meas}}/\text{NH}_4^+_{\text{neu}} \geq 1$), since the dissociation reactions of NH_4^+ and water are not currently included in the AIM model and since the pH of near neutralized particles would be strongly influenced by the presence of weaker acids and bases. However, $\text{mH}^+_{\text{aq}} < 0$ can result if a fraction of the excess NH_4^+ is due to the neutralization of organic acids by NH_4^+ (also see Section 4.1.).

3.4. Size Resolved H^+_{Aer} and $\text{NH}_4^+_{\text{meas}}/\text{NH}_4^+_{\text{neu}}$. The size-resolved H^+_{Aer} concentration and $\text{NH}_4^+_{\text{meas}}/\text{NH}_4^+_{\text{neu}}$ ratio are estimated from the AMS size distributions of NH_4^+ , SO_4^{2-} , and NO_3^- based on eqs 1 and 2. Cl^- was not scanned for size distributions during this study; but this omission is negligible because Cl^- typically accounts for <1% of the total equivalent

TABLE 1. Statistics of H^+_{Aer} Concentrations (eq 1) and Measured-to-Neutralized NH_4^+ Ratio (eq 2) during the Entire Study Period ($N = 3599$), Acidic Particle Periods ($N = 1033$), and Neutralized Particle Periods ($N = 669$)

	$NH_4^+_{meas}/NH_4^+_{neu}$			H^+_{Aer} (nmol m ⁻³)		
	entire study	acidic	neutralized	entire study	acidic	neutralized
mean	0.89	0.69	0.99	28	79	0.8
1s	0.21	0.10	0.06	41	46	7.2
median	0.88	0.71	0.99	15	77	0.7
90th	1.13	0.81	1.1	88	140	9.2
75th	0.99	0.76	1.0	44	109	4.6
25th	0.76	0.64	0.96	0.8	43	-2.8
10th	0.65	0.57	0.92	-8.2	18	-7.1

concentrations of the anions in Pittsburgh (11). The size distributions of NH_4^+ and SO_4^{2-} were derived from the particle time-of-flight measurements of their main ions from the AMS after two corrections: (1) The size distributions of NH_4^+ were corrected for the penetration of gas-phase O^+ signal (mainly from O_2) into the particle region, and were adjusted for faster flight of the NH_2^+ ion in the quadrupole mass spectrometer compared to the ions of sulfate and nitrate (11, 27); (2) The size distributions of SO_4^{2-} were corrected for slightly elevated baselines at larger sizes—a result of relatively slower evaporation of sulfate compounds compared to the other species.

4. Results and Discussion

4.1. H^+_{Aer} and $NH_4^+_{meas}/NH_4^+_{neu}$. Table 1 summarizes the statistics of the H^+_{Aer} concentration and the $NH_4^+_{meas}/NH_4^+_{neu}$ ratio. Submicrometer particles are, on average, acidic in Pittsburgh during this study. Episodes of “more acidic” particles ($NH_4^+_{meas}/NH_4^+_{neu} < 0.75 + 1\sigma$, i.e., the molar ratio of NH_4HSO_4 to $(NH_4)_2SO_4 > 1$), occur ~30% of the time. The mean ($\pm 1\sigma$) mole equivalent concentration of H^+_{Aer} is 28 ± 41 nmol m⁻³ (median = 15 nmol m⁻³; Table 1), comparable to the average H^+_{Aer} concentrations observed at various sites, including New York City (16), Toronto, Buffalo, and several other U.S. sites (15, 18, and references therein). Higher fine particle concentrations of H^+_{Aer} (up to 5 times larger) are seen in Hong Kong (4, 18) and India (14), where ambient air is more strongly influenced by local and regional SO_2 emissions.

The H^+_{Aer} concentrations correlate well to those of SO_4^{2-} ($r^2 = 0.68$; Figure 1). The linear fit slope indicates that the bulk submicrometer particles during this study are either partially or fully neutralized by ammonium and that, on average, bisulfate appears to be the most acidic form of sulfate in these particles. This observation is consistent with an earlier study in Pittsburgh that aerosols are a mixture of $(NH_4)_2SO_4$ and NH_4HSO_4 with very little H_2SO_4 during acidic episodes (28).

There is very little nitrate in acidic particles during relatively high SO_4^{2-} periods (Figure 1). We estimate that the average concentration of organic acids in fine particles is approximately 2–5 nmol m⁻³, based on the mass ratio of six major organic acids measured by GC-MS to AMS m/z 44 (ratio = 0.85 ± 0.04) observed in PM_1 during summer 2003 in Tokyo, Japan (the average molecular weight of these organic acids is ~100 g mol⁻¹ (29)). These facts together indicate that the aerosol acidity in Pittsburgh is mainly related to SO_4^{2-} with very little overall contribution from NO_3^- , Cl^- , and organic acids.

4.2. Temporal variations of particle acidity measures.

Shown in Figure 2b–d are the time series of acidity indicators, H^+_{Aer} concentration, $NH_4^+_{meas}/NH_4^+_{neu}$, and pH. Both H^+_{Aer} and $NH_4^+_{meas}/NH_4^+_{neu}$ are dependent on the mass concentration of SO_4^{2-} (Figures 1 and 2e). Episodes with high SO_4^{2-}

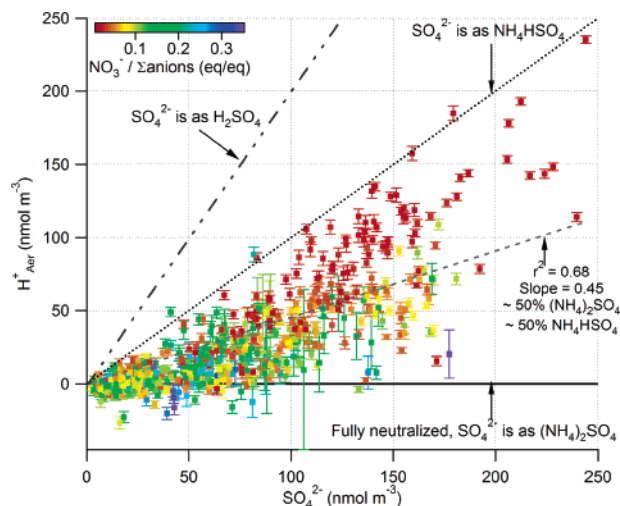


FIGURE 1. Scatter plot that compares the concentrations of H^+_{Aer} to SO_4^{2-} in submicrometer particles, colored by the equivalent ratio of NO_3^- to total anions, during September 7–22, 2002 in Pittsburgh. The error bars were calculated based on error propagation of the measurement uncertainties and noise for NH_4^+ , SO_4^{2-} , Cl^- , and NO_3^- . To reduce clutter, only every fifth of the data points in time are shown.

(>100 nmol m⁻³) are generally less neutralized than those with lower SO_4^{2-} (<100 nmol m⁻³). Figure 2e indicates that abnormally high $NH_4^+_{meas}/NH_4^+_{neu}$ values are due to low signal-to-noise for the detected ions.

The trend in pH is consistent with that of $NH_4^+_{meas}/NH_4^+_{neu}$, although the variations in pH are larger (see Supporting Information Figure S1) because pH (and ionic strength) is also strongly influenced by changes in ambient humidity (15–96%; average $\pm 1\sigma = 63\% \pm 22\%$ during this study). In addition, the measured RH values, which represent the instantaneous value in ambient air, do not reflect the RH history of the particles. We thus investigate the direct correlation between $NH_4^+_{meas}/NH_4^+_{neu}$ and pH modeled under constant RH (80%, the deliquescence RH of $(NH_4)_2SO_4$) and T (295 K) conditions. The tight correlation between the pH and $NH_4^+_{meas}/NH_4^+_{neu}$ ($r = 0.96$; Figure S1c) confirms that it is reasonable to use the $NH_4^+_{meas}/NH_4^+_{neu}$ ratio as an acidity indicator for the separation of the neutralized and acidic particle periods (Figure 2d).

The diurnal patterns of the pH, the H^+_{Aer} concentration, and the $NH_4^+_{meas}/NH_4^+_{neu}$ ratio all indicate that particles are most acidic in the afternoon (see Supporting Information Figure S2). These trends are consistent with the reduction in particle water content (due to lower RH) in the afternoon and the hypothesis that more intense photochemistry and oxidation of SO_2 in the afternoon (over regional scales) leads to more acidic particles.

4.3. Average and Time-Resolved Size Distributions of

H^+_{Aer} and $NH_4^+_{meas}/NH_4^+_{neu}$. The average size distribution of H^+_{Aer} peaks at the same diameter ($D_{va}(30) \approx 500 - 600$ nm) as those of inorganic and total mass (Figure 3). This is consistent with the facts that (1) H^+_{Aer} correlates with SO_4^{2-} mass concentration (Figures 1 and 2d–e) and (2) the relative SO_4^{2-} mass loading in 500–600 nm particles increase during “acidic” time periods compared to “neutralized” periods (see Figure 6a and associated discussion below). Since this 500–600 nm accumulation mode is largely made up of aged regional aerosol particles rich in sulfate and oxidized organics (11, 27), the peak H^+_{Aer} concentration in this mode indicates that there is generally not enough gas-phase NH_3 to completely neutralize sulfate on a regional scale in the Pittsburgh region. This conclusion is also consistent with the observation that aerosols from high SO_4^{2-} loading periods tend to be more acidic (Figure 2d–e).

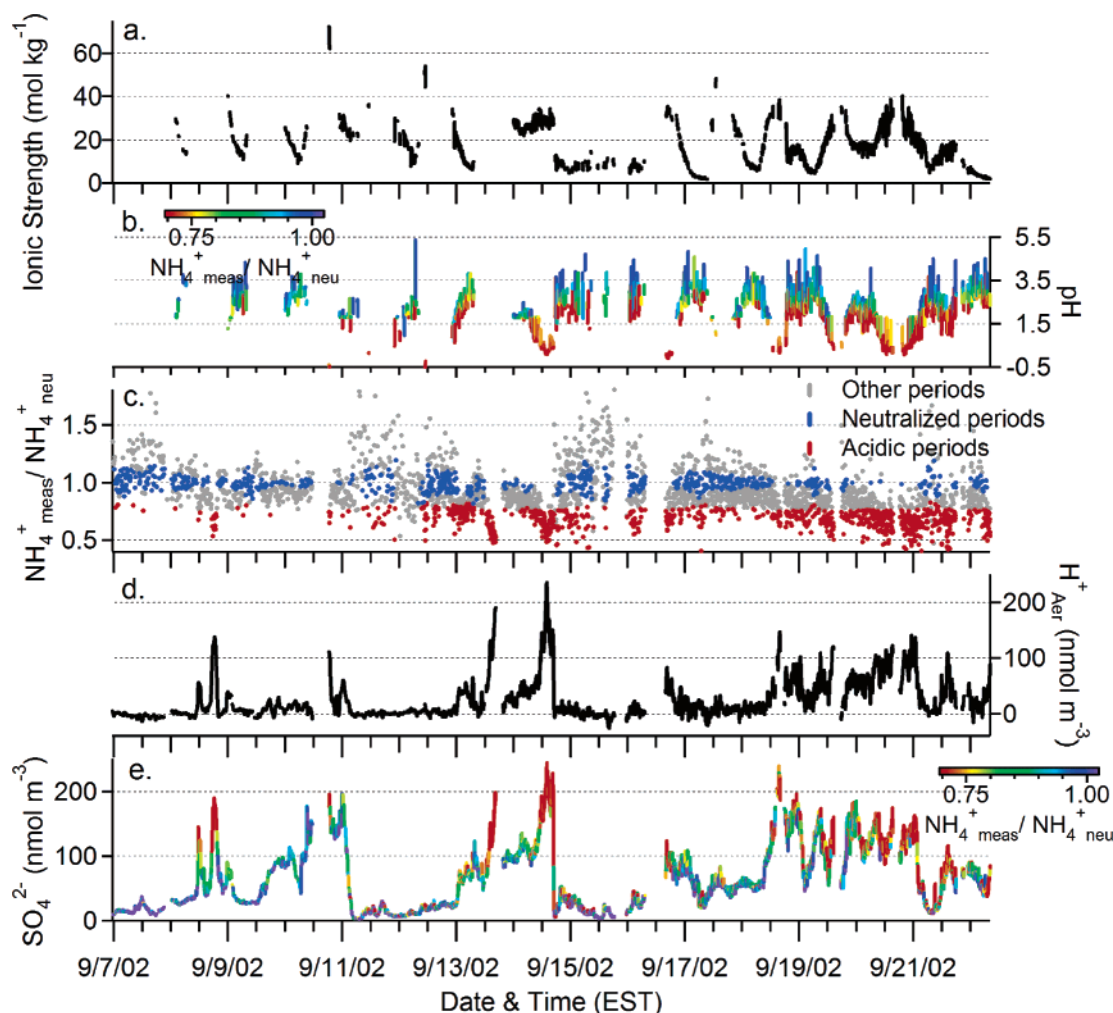


FIGURE 2. Time series of (a) ionic strength, (b) pH, (c) $\text{NH}_4^+_{\text{meas}}/\text{NH}_4^+_{\text{neu}}$ ratio, (d) H^+_{Aer} concentration, and (e) SO_4^{2-} concentration in submicrometer particles in Pittsburgh. The $\text{NH}_4^+_{\text{meas}}/\text{NH}_4^+_{\text{neu}}$ curve is colored by periods of more acidic aerosol (red), bulk neutralized (green), and the rest that fall into a mildly acidic regime (gray) classified based on criteria described in section 3. Both the pH and the SO_4^{2-} curves are colored by $\text{NH}_4^+_{\text{meas}}/\text{NH}_4^+_{\text{neu}}$ ratios. Ionic strength and pH are calculated from the AIM model under ambient T and RH conditions. Reasons for missing data points in pH and ionic strength compared to the other three are explained in Section 3.3. Note that the unit of the ionic strength is mole of ions per kilogram of particle phase water.

In addition to the 500–600 nm mode, the H^+_{Aer} distribution also shows a mode at $D_{va} \sim 200$ nm, which likely results from condensed freshly formed H_2SO_4 because (1) This mode evolves more noticeably in the afternoon (Figure 4); (2) The small mode particles are more acidic than the larger particles according to $\text{NH}_4^+_{\text{meas}}/\text{NH}_4^+_{\text{neu}}$ (Figures 3b); and (3) Very acidic ultrafine particles were detected during the frequent new particle formation and growth events in Pittsburgh (27). A comparison of the average diurnal evolution of the H^+_{Aer} size distribution during days with new particle formation and growth events to that during days without (see Supporting Information Figure S3) provide additional support to these points.

There is strong evidence that the formation and growth of new particles in Pittsburgh are tightly linked to SO_2 photooxidation and thus H_2SO_4 production (27, 31). Indeed, the best correlation of SO_2 is found with the small mode sulfate particles (see Supporting Information Figure S4), as condensation of fresh H_2SO_4 to smaller particles is faster due to the reduced diffusion limitation compared to larger particles. Thus, the lack of stoichiometric neutralization in the 200 nm mode is likely caused by the slow mixing of gas-phase NH_3 into SO_2 rich plumes.

4.4. Influence of Particle Acidity on Organic Aerosols. We recently developed a multivariate data analysis technique

(22) that yields the concentrations, size distributions, and mass spectra of oxygenated (OOA) and hydrocarbon-like (HOA) organic aerosols (23). OOA appears to be a good surrogate for SOA during this study and HOA is dominated by POA from combustion emissions (23). On average, the Pittsburgh organic aerosol consists of 65% OOA and 35% HOA. Given their very different time trends, mass spectra, and size distributions, the separation of the HOA and OOA signals represents a crucial step in any detailed analysis of the relationship between particle acidity and SOA formation in Pittsburgh.

The mass loadings of OOA and sulfate are tightly correlated ($r^2 = 0.74$; Figure 5) and their size distributions are very similar, suggesting that SOA and SO_4^{2-} are internally mixed and are both formed over regional scales (12, 23), with a possible contribution of cloud processing to both. The average OOA to SO_4^{2-} ratio is 0.49 and $0.33 \mu\text{g m}^{-3}/\mu\text{g m}^{-3}$, respectively, in bulk neutralized and more acidic particles (see Supporting Information Figure S5). This difference suggests that SO_4^{2-} is added faster than OOA to acidic aerosols, possibly due to faster gas-phase or cloud production, and/or higher concentration of SO_2 than of OOA gas-phase precursors on those airmasses. Recent laboratory studies on sulfate aerosols of much higher acidity than observed in this study report the formation of organosulfate species (32). Although we cannot

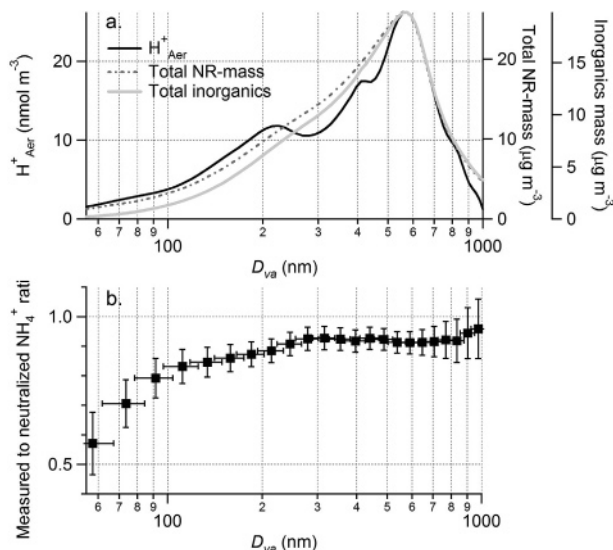


FIGURE 3. Average size distributions ($dX/d\log D_{va}$) of (a) H^+_{Aer} , total mass, and total inorganic concentrations and (b) $NH_4^+_{meas}/NH_4^+_{neu}$ ratio in submicrometer particles during September 7–22, 2002 in Pittsburgh. A 3-point binning was applied to the size distribution of $NH_4^+_{meas}/NH_4^+_{neu}$ to reduce high-frequency noise. The vertical error bars in Figure 3b were calculated based on error propagation of the measurement uncertainties and noise for NH_4^+ , SO_4^{2-} , and NO_3^- size distributions. The horizontal error bars are uncertainties in AMS size measurement estimated from the finite chopper opening and particle vaporization times ($\sim 50 \mu s$).

rule out the presence of these species in the acidic particles we do not observe any clear evidence of their presence.

In comparison, the size distributions of both SO_4^{2-} and OOA in the 600 nm mode are enhanced during acidic time periods, while SO_4^{2-} is also enhanced at the 200 nm mode (Figure 6a). The average concentrations of SO_4^{2-} and OOA during acidic periods are 100 and 25% higher, respectively, compared to neutralized periods. Since the acidic time periods are more prevalent in the afternoon (Figure 6b), it is possible that the higher average OOA concentration during acidic periods is due to increased SOA photochemical production (with or without the effects of acid-catalysis). Cloud processing may also affect the observed OOA concentration in the 600 nm mode. Thus, the strongest evidence for the lack of strong acidity dependent SOA formation is provided by the 200 nm mode, where cloud processing should be less important.

If we attribute the entire difference in OOA between neutralized and “more acidic” periods to acid-catalyzed SOA formation, the upper bound increase of SOA mass (normalized by the diurnal variation of OOA concentrations) that could be due to this mechanism is estimated at 25%. While this analysis is limited by the uncertainty of comparing different time periods during a relatively short study, an important result is the lack of very large acidity-related enhancements of SOA (e.g., several fold) that was observed in some chamber studies (5, 6) and inferred in industrial plumes (9). Note that other recent laboratory studies report much more moderate increases (10–40%) of SOA on acidic seed particles (7, 8, 17). One possible reason for the observed differences in acidity dependent SOA yield is that $NH_4^+_{meas}/NH_4^+_{neu}$ ratio of the seed particles used in the studies by Jang et al. (5) was lower (~ 0.41) than measured for the average acidic particle in Pittsburgh (0.69; Table 1). According to AIM, the average pH in the acidic particles analyzed in this study

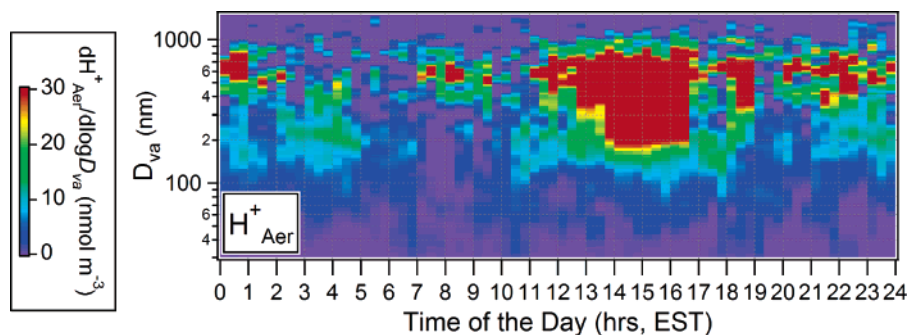


FIGURE 4. Average daily evolution of the size distribution of H^+_{Aer} concentration during September 7–22, 2002

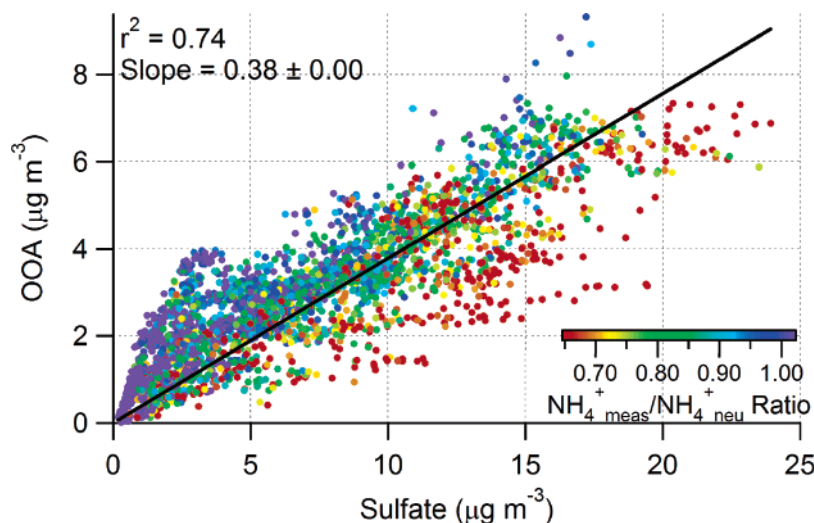


FIGURE 5. Scatter plot of mass concentrations of oxygenated organic aerosol vs sulfate during September 7–22, 2002. The traces are colored by $NH_4^+_{meas}/NH_4^+_{neu}$ to show how this correlation varies as a function of ammonium deficit.

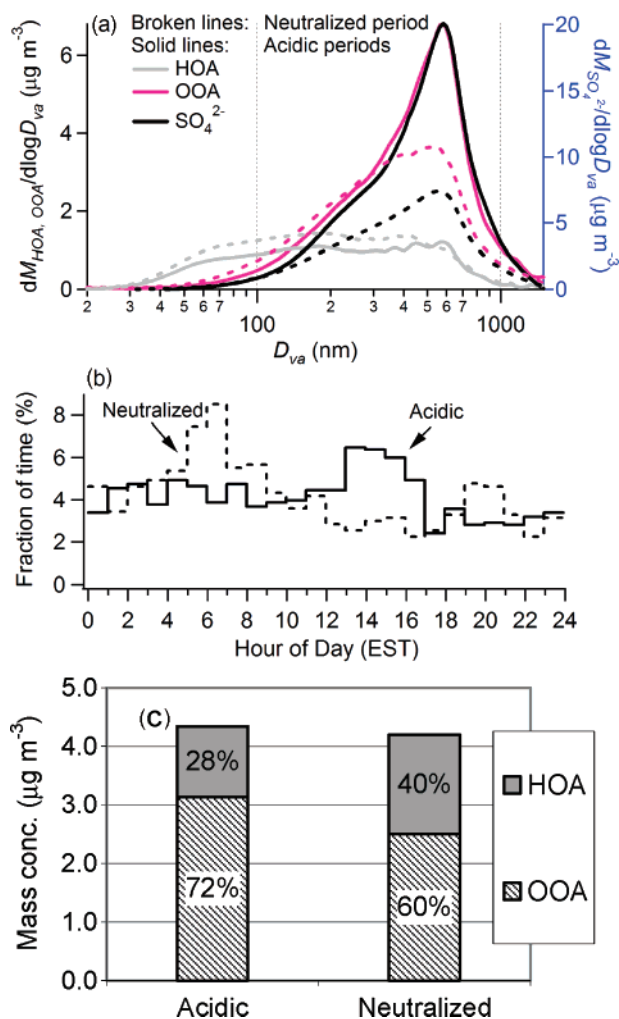


FIGURE 6. (a) Average size distributions of OOA, HOA, and SO₄²⁻ during periods dominated by bulk neutralized aerosols (broken lines) and by more acidic aerosols (solid lines), (b) the occurrence frequencies of these two periods, and (c) the average mass fractionations of HOA and OOA during them.

is more than 2 units higher (i.e., the concentration of free H⁺ relative to aerosol phase water content is ~100 times lower) than the pH of the seed aerosols used in the chamber study by Jang et al. (5) (see Supporting Information Figure S6). Acid-catalyzed SOA formation could be more important in rural locations where particles are sometimes more acidic than observed in this study (e.g., ref 28). However, note that in our earlier analysis of particle chemistry during the nucleation events in Pittsburgh, we did not find evidence for the acid-related SOA enhancement either in the more acidic (NH₄⁺_{meas}/NH₄⁺_{neu} of ~0.58) ultrafine particles (23, 27).

The mass spectra of HOA and OOA extracted independently for the acidic and neutralized aerosol periods are almost identical (see Supporting Information Figure S7), suggesting similarities in aerosol chemical compositions, despite the significant differences in particle acidity. The OOA spectrum during “more acidic” periods shows a slightly lower relative signal intensity at larger *m/z*'s (>200 amu) compared to that of neutralized periods (Figure S7), indicating that SOA oligomers are not more prevalent during the acidic periods in Pittsburgh. While oligomers would experience significant fragmentation in the AMS due to the relatively “hard” vaporization and ionization conditions, smog chamber experiments have shown that oligomers in isoprene SOA still produce clear signals in the AMS at higher *m/z* ratios (33).

A recent study by Kroll et al. (34) suggests that the ionic strength (*I*), rather than the acidity, of the seed aerosols may be responsible for the observed large enhancement of SOA mass in chamber studies. It is difficult to differentiate this effect from the influence of aerosol acidity (pH) in this study since the pH and *I* are well anticorrelated (Figure 2) due to the dominant effect of RH. The average *I* from the more acidic periods is higher (~24 mol kg⁻¹ of particle phase water vs ~14 mol kg⁻¹ from the neutralized periods). For the influence of these two parameters on SOA formation to be evaluated separately, the techniques used here should be applied to data from an area and time period where *I* and pH are not strongly correlated.

Acknowledgments

We thank Drs. B. Wittig (CUNY) and S. Pandis for meteorological data and F. SanMartini (NAS) and R. Volkamer (MIT) for helpful discussions on AIM. This work was supported by the startup funding from SUNY-Albany for QZ, and by the U.S. EPA STAR grant R832161010, NASA grant NNG04GA67G, and NSF CAREER grant ATM-0449815. Although this work has been partly funded by EPA and NSF, it has not been subjected to either agency's review and therefore does not necessarily reflect the views of the agencies and no official endorsement should be inferred.

Supporting Information Available

Additional detail is shown in seven figures. This material is available free of charge via the Internet at <http://pubs.acs.org>.

Literature Cited

- Utell, M. J.; Looney, R. J. Environmentally induced asthma. *Toxicol. Lett.* **1995**, *82/83*, 47–53.
- Likens, G. E.; Driscoll, C. T.; Buso, D. C. Long-term effects of acid rain: Response and recovery of a forest ecosystem. *Science* **1996**, *272*, 244–246.
- Khlystov, A.; Stanier, C. A.; Takahama, S.; Pandis, S. N. Water content of ambient aerosol during the Pittsburgh air quality study. *J Geophys Res., [Atmos]* **2005**, *110*.
- Pathak, R. K.; Louie, P.; Chan, C. K. Characteristics of aerosol acidity in Hong Kong. *Atmos. Environ.* **2004**, *38*, 2965–2974.
- Jang, M. S.; Czoschke, N. M.; Sangdon, L.; Kamens, R. M. Heterogeneous atmospheric aerosol production by acid-catalyzed particle-phase reactions. *Science* **2002**, *298*, 814–817.
- Edney, E. O.; Kleindienst, T. E.; Jaoui, M.; Lewandowski, M.; Offenberg, J. H.; Wang, W.; Claeys, M. Formation of 2-methyl tetrols and 2-methylglyceric acid in secondary organic aerosol from laboratory irradiated isoprene/NO_x/SO₂/air mixtures and their detection in ambient PM_{2.5} samples collected in the eastern United States. *Atmos. Environ.* **2005**, *39*, 5281–5289.
- Gao, S.; Keywood, M.; Ng, N. L.; Surratt, J.; Varutbangkul, V.; Bahreini, R.; Flagan, R. C.; Seinfeld, J. H. Low-molecular-weight and oligomeric components in secondary organic aerosol from the ozonolysis of cycloalkenes and alpha-pinene. *J. Phys. Chem. A* **2004**, *108*, 10147–10164.
- Iinuma, Y.; Boge, O.; Miao, Y.; Sierau, B.; Gnauk, T.; Herrmann, H. Laboratory studies on secondary organic aerosol formation from terpenes. *Faraday Discuss.* **2005**, *130*, 279–294.
- Brock, C. A.; Trainer, M.; Ryerson, T. B.; Neuman, J. A.; Parrish, D. D.; Holloway, J. S. Particle growth in urban and industrial plumes in Texas. *J Geophys Res. [Atmos]* **2003**, *108*, 4111.
- Chu, S.-H. PM_{2.5} episodes as observed in the speciation trends network. *Atmos. Environ.* **2004**, *38*, 5237–5246.
- Zhang, Q.; Canagaratna, M. R.; Jayne, J. T.; Worsnop, D. R.; Jimenez, J.-L. Time and size-resolved chemical composition of submicron particles in Pittsburgh - Implications for aerosol sources and processes. *J. Geophys. Res.* **2005**, *110*, doi:10.1029/2004JD004649.
- Takahama, S.; Davidson, C. I.; Pandis, S. N. Semicontinuous measurements of organic carbon and acidity during the Pittsburgh air quality study: Implications for acid-catalyzed organic aerosol formation. *Environ. Sci. Technol.* **2006**, *40*, 2191–2199.
- Pathak, R. K.; Yao, X.; Chan, C. K. Sampling artifacts of acidity and ionic species in PM_{2.5}. *Environ. Sci. Technol.* **2004**, *38*, 254–259.

- (14) Mouli, P. C.; Mohan S. V.; Reddy, S. J. A study on major inorganic ion composition of atmospheric aerosols at Tirupati. *J. Hazard. Mater.* **2003**, *96*, 217–228.
- (15) Thurston, G. D.; Gorczynski, J. E. Jr.; Currie, J. H.; He, D.; Ito, K.; Hipfner, J.; Waldman, J.; Lioy, P. J.; Lippmann, M. The nature and origins of acid summer haze air pollution in metropolitan Toronto, Ontario. *Environ. Res.* **1994**, *65*, 254–270.
- (16) Hogrefe, O.; Schwab, J. J.; Drewnick, F.; Lala, G. G.; Peters, S.; Demerjian, K. L.; Rhoads, K.; Felton, H. D.; Rattigan, O. V.; Husain, L.; Dutkiewicz, V. A. Semicontinuous PM_{2.5} sulfate and nitrate measurements at an urban and a rural location in New York: PMTACS-NY summer 2001 and 2002 campaigns. *J. Air Waste Manage. Assoc.* **2004**, *54*, 1040–1060.
- (17) Czoschke, N. M.; Jang, M. Acidity effects on the formation of a-pinene ozone SOA in the presence of inorganic seed. *Atmos. Environ.* **2006**, *40*, 4370–4380.
- (18) Pathak, R. K.; Lau, A. K. H.; Chan, C. K. Acidity and concentrations of ionic species of PM_{2.5} in Hong Kong. *Atmos. Environ.* **2003**, *37*, 1113–1124.
- (19) Cabada, J. C.; Rees, S.; Takahama, S.; Khlystov, A.; Pandis, S. N.; Davidson, C. I.; Robinson, A. L. Mass size distributions and size resolved chemical composition of fine particulate matter at the Pittsburgh Supersite. *Atmos. Environ.* **2004**, *38*, 3127–3141.
- (20) Wittig, A. E.; Anderson, N.; Khlystov, A. Y.; Pandis, S. N.; Davidson, C.; Robinson, A. L. Pittsburgh Air Quality Study overview and initial scientific findings. *Atmos. Environ.* **2004**, *38*, 3107–3125.
- (21) Clegg, S. L.; Brimblecone, P.; Wexler, A. S. A thermodynamic model of the system $\text{H}^+ - \text{NH}_4^+ - \text{SO}_4^{2-} - \text{NO}_3^- - \text{H}_2\text{O}$ at tropospheric temperatures. *J. Phys. Chem. A* **1998**, *102*, 2137–2154.
- (22) Zhang, Q.; Alfarra, M. R.; Worsnop, D. R.; Allan, J. D.; Coe, H.; Canagaratna, M. R.; Jimenez, J. L. Deconvolution and quantification of hydrocarbon-like and oxygenated organic aerosols based on aerosol mass spectrometry. *Environ. Sci. Technol.* **2005**, *39*, 4938–4952, doi:10.1021/es048568l.
- (23) Zhang, Q.; Worsnop, D. R.; Canagaratna, M. R.; Jimenez, J. L. Hydrocarbon-like and oxygenated organic aerosols in Pittsburgh: Insights into sources and processes of organic aerosols. *Atmos. Chem. Phys.* **2005**, *5*, 3289–3311.
- (24) Volkamer, R.; Jimenez, J. L.; Martini, F. S.; Dzepina, K.; Zhang, Q.; Salcedo, D.; Molina, L. T.; Molina, M. J.; Worsnop, D. R. Secondary organic aerosol formation from anthropogenic VOCs: Rapid and higher than expected. *Geophys. Res. Lett.* **2006**, *33*, doi:10.1029/2006GL026899.
- (25) Kleinman, L. I.; Daum, P. H.; Lee, Y.-N.; Senum, G. I.; Springston, S. R.; Wang, J.; Berkowitz, C.; Hubbe, J.; Zaveri, R. A.; Brechtel, F. J.; Jayne, J.; Onasch, T. B.; Worsnop, D. Aircraft observations of aerosol composition in New England and mid-Atlantic states during the summer 2002 NEAQS field campaign. *J. Geophys. Res.* **2006**, submitted.
- (26) Ansari, A. S.; Pandis, S. N. Water absorption by secondary organic aerosol and its effect on inorganic aerosol behavior. *Environ. Sci. Technol.* **2000**, *34*, 71–77.
- (27) Zhang, Q.; Stanier, C. O.; Canagaratna, M. R.; Jayne, J. T.; Worsnop, D. R.; Pandis, S. N.; Jimenez, J. L. Insights into the chemistry of new particle formation and growth events in Pittsburgh based on Aerosol Mass Spectrometry. *Environ. Sci. Technol.* **2004**, *38*, 4797–4809.
- (28) Liu, L.-J. S.; Burton, R.; Wilson, W. E.; Koutrakis, P. Comparison of aerosol acidity in urban and semi-rural environments. *Atmos. Environ.* **1996**, *30*, 1237–1245.
- (29) Takegawa, N.; Miyakawa, T.; Kawamura, K.; Kondo, Y. Contribution of selected dicarboxylic and ω -oxocarboxylic acids in ambient aerosol to m/z 44 signal of an Aerodyne Aerosol Mass Spectrometer. *Aerosol Sci. Tech.* **2007**, in press.
- (30) DeCarlo, P. F.; Slowik, J. G.; Worsnop, D. R.; Davidovits, P.; Jimenez, J. L. Particle morphology and density characterization by combined mobility and aerodynamic diameter measurements. Part 1: Theory. *Aerosol Sci. Technol.* **2004**, *38*, 1185–1205.
- (31) Stanier, C.; Khlystov, A.; Pandis, S. N. Nucleation events during the Pittsburgh Air Quality Study: Description and relation to key meteorological, gas phase, and aerosol parameters. *Aerosol Sci. Technol.* **2004**, 253–264.
- (32) Liggio, J.; Li, S.-M. Organosulfate formation during the uptake of pinonaldehyde on acidic sulfate aerosols. *Geophys. Res. Lett.* **2006**, *33*, No. 13, doi:10.1029/2006GL026079.
- (33) Kroll, J. H.; Ng, N. L.; Murphy, S. M.; Flagan, R. C.; Seinfeld, J. H. Secondary Organic Aerosol Formation from Isoprene Photooxidation. *Environ. Sci. Technol.* **2006**, *40*, 1869–1877.
- (34) Kroll, J. H.; Ng, N. L.; Murphit, S. M.; Varutbangkul, V.; Flagan, R. C.; Seinfeld, J. H. Chamber studies of secondary organic aerosol growth by reactive uptake of simple carbonyl compounds. *J. Geophys. Res. [Atmos]* **2005**, 110.

Received for review July 31, 2006. Revised manuscript received November 18, 2006. Accepted January 4, 2007.

ES061812J

575 **A Case Study of Urban Particle Acidity and Its Influence on Secondary Organic Aerosol**
576 **(Supplementary Information)**

577

578 Qi Zhang^{1*}, Jose-Luis Jimenez², Douglas R. Worsnop³, and Manjula Canagaratna³

579

580 ¹Atmospheric Sciences Research Center (ASRC) and Department of Environmental Health
581 Sciences

582 251 Fuller Road, CESTM L110

583 University at Albany, State University of New York, Albany, NY 12003

584

585 ²Cooperative Institute for Research in Environmental Sciences (CIRES) and Department of

586 Chemistry and Biochemistry

587 216 UCB

588 University of Colorado-Boulder

589 Boulder, Colorado 80309

590

591 ³Aerodyne Research Inc

592 Billerica, Massachusetts 01821

593

594 * Author to whom correspondence should be addressed.

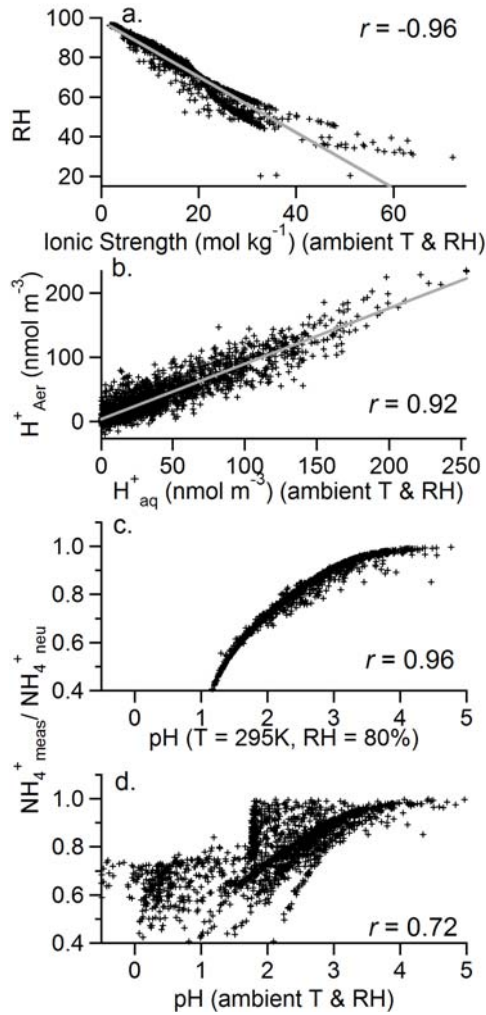
595 E-mail: qz@asrc.cestm.albany.edu

596 Tel: (518) 437-8752; Fax: (518) 437-8758

597

598

599 Figure S1. Scatter plots of a) RH vs. AIM II modeled ionic strength (Eqn. 4), b) H^+_{Aer}
600 concentration from ion balance (Eqn. 1) vs. AIM II modeled total H^+ concentration (H^+_{aq}) under
601 ambient T and RH, c) $NH_4^+_{meas}/NH_4^+_{neu}$ ratio (Eqn. 2) vs. AIM II modeled pH (Eqn. 3) assuming
602 constant temperature and RH conditions, and d) $NH_4^+_{meas}/NH_4^+_{neu}$ ratio vs. AIM II modeled pH
603 under ambient conditions in submicron particles in Pittsburgh.



660
661
662
663

664 Figure S2. Diurnal variations of a) the mass concentration of H^+ ion (Equation 1); b) the ratio of
 665 measured to needed-for-neutralization NH_4^+ concentration (Equation 2); c) ionic strength
 666 calculated from the output of the AIM-II model (Equation 4), and d) pH (Equation 3) calculated
 667 from the output of the AIM-II model, for submicron particles during September 7 – 22, 2002 in
 668 Pittsburgh. Note that the diurnal variations of ionic strength (Figure S2c) and pH (Figure S2d)
 669 are only for periods (as shown in Figure 2) when AIM-II gives valid outputs, i.e., when particles
 670 are neither bulk neutralized based on ionic balance nor completely dry
 672

674

676

678

680

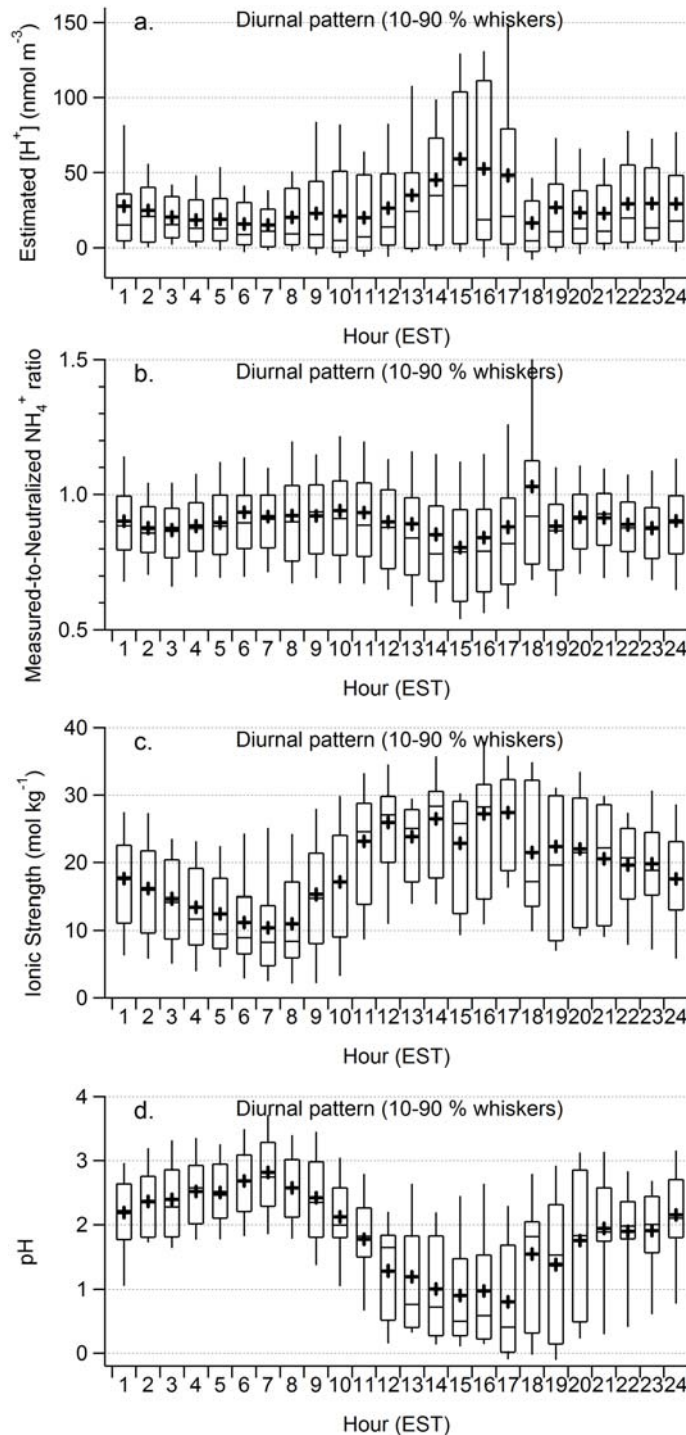
682

684

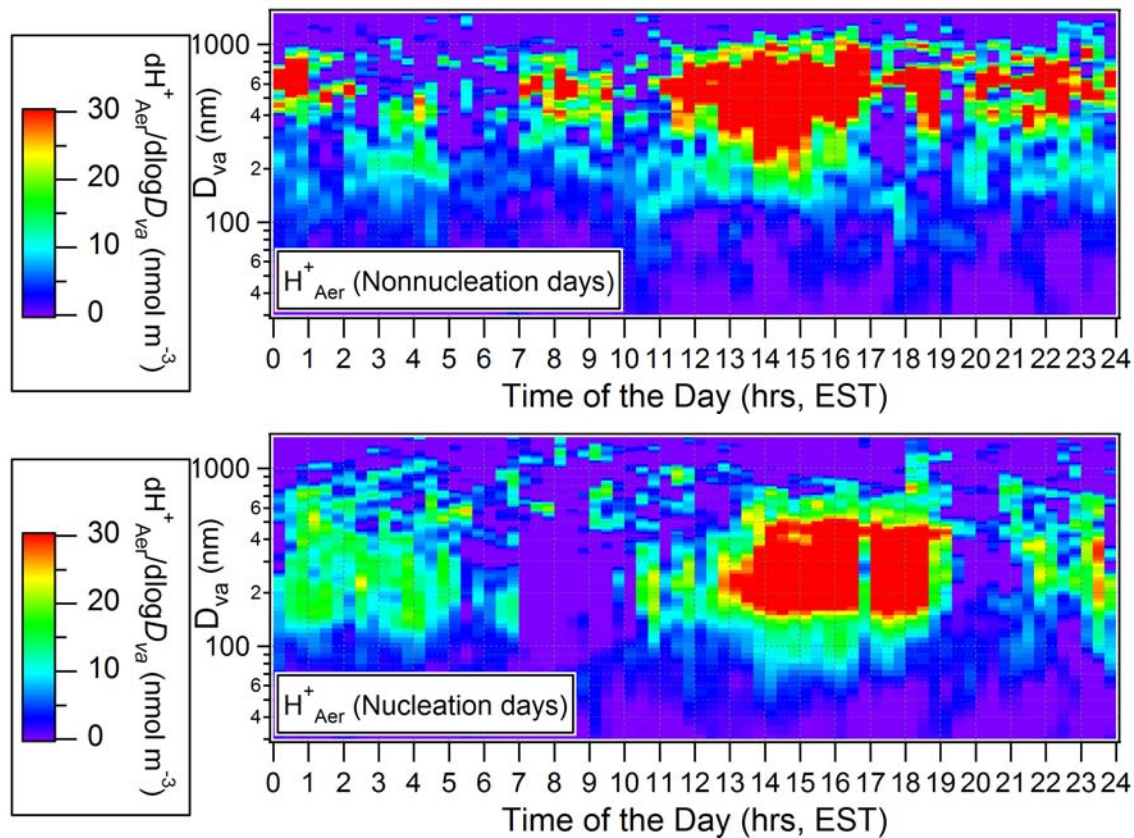
686

688

690

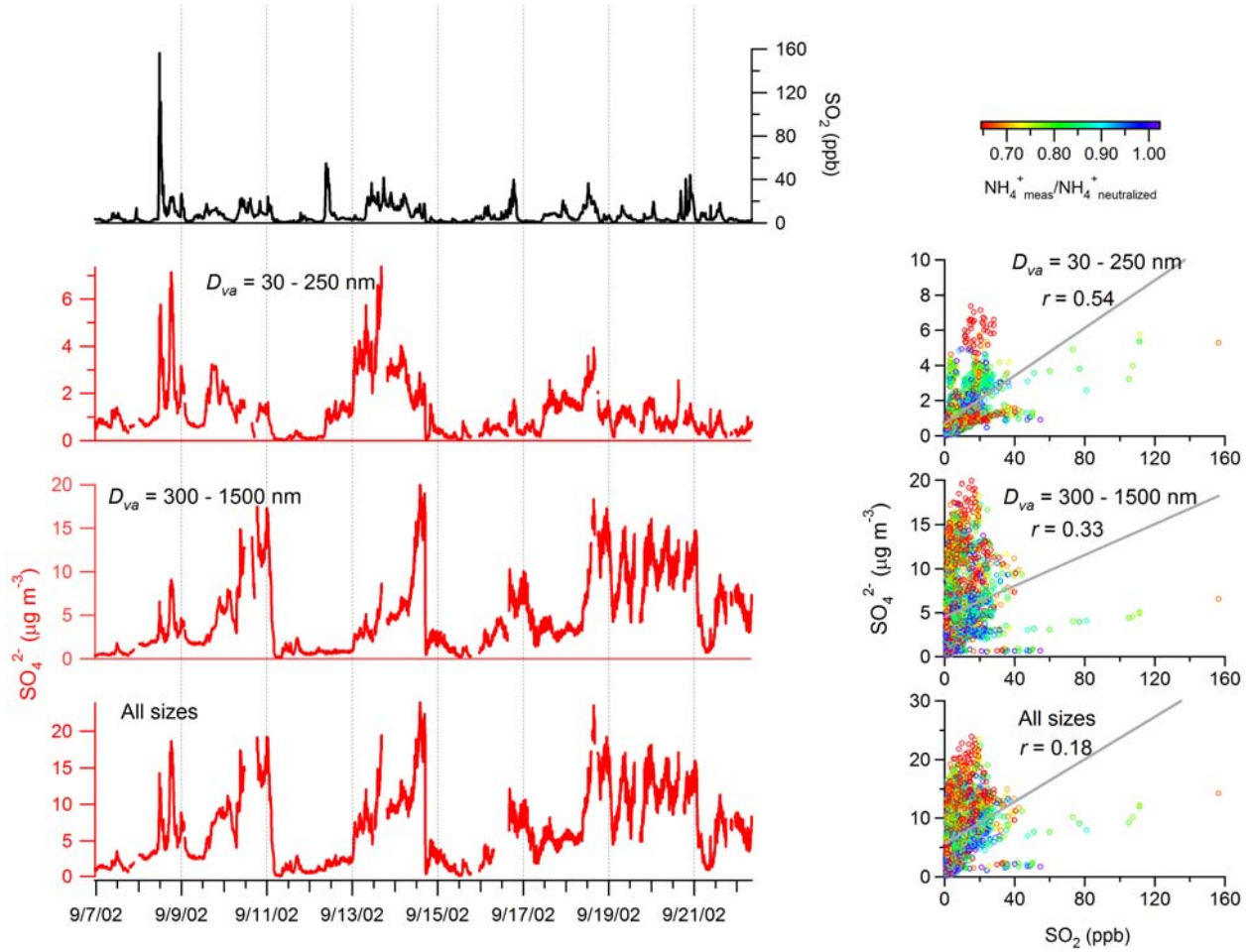


691 Figure S3 Average daily evolution of the size distribution of H^+_{Aer} concentration during days
692 without new particle formation and growth events and days with (September 7, 8, 9, 12, 13,
693 2002) (27).

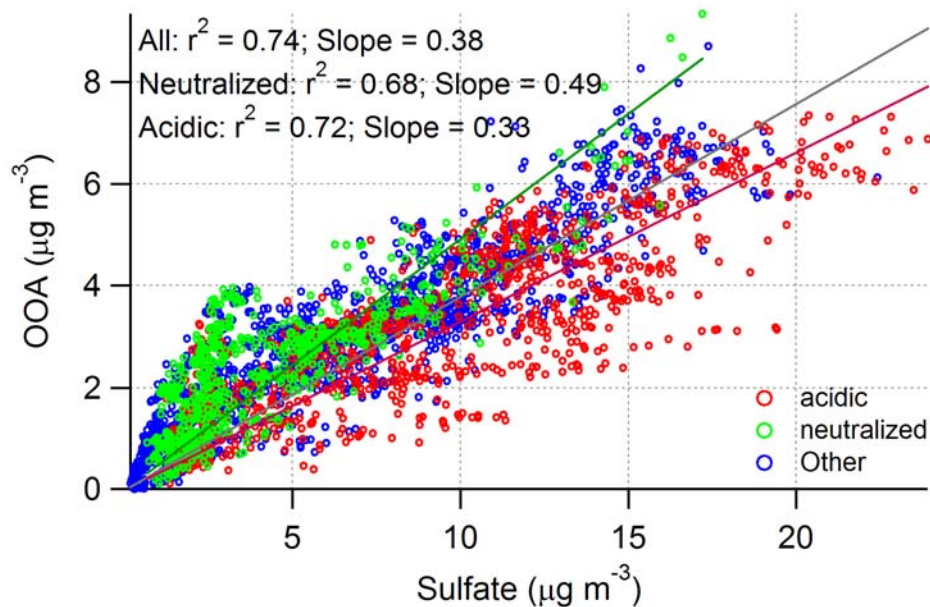


694
695
696
697

Figure S4. Time series of SO₂ and sulfate (for different particle size bins) and the corresponding correlation plots of sulfate vs. SO₂.

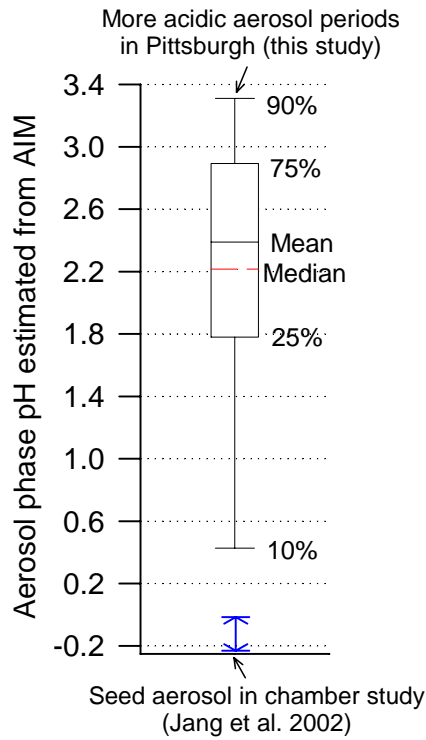


698 Figure S5. Scatter plot that shows the correlation between the mass concentrations of
699 oxygenated organic aerosol and sulfate during September 7 – 22, 2002. The traces are colored
700 according to the identification of the period as acidic, neutralized, or other.

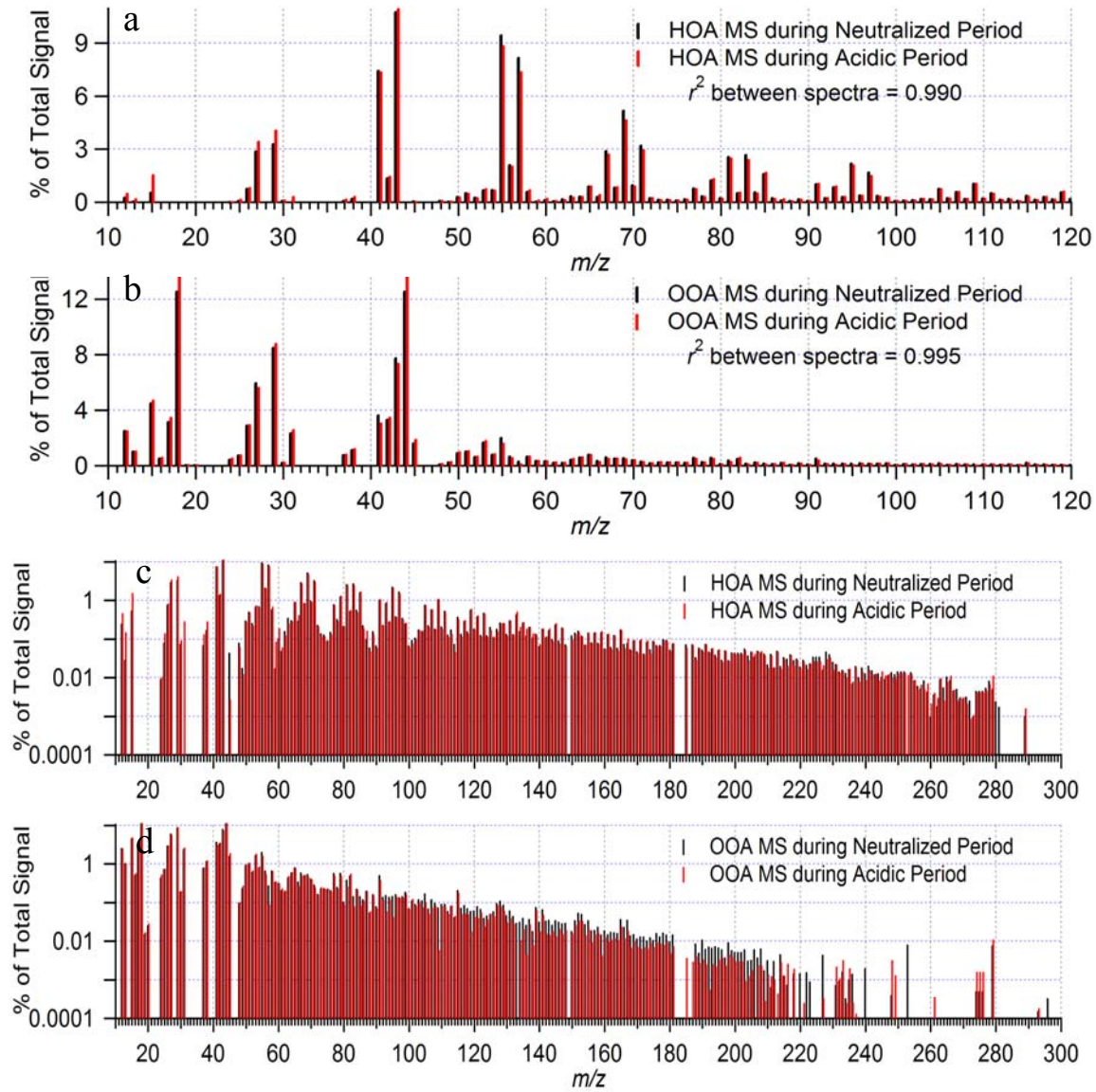


720 Figure S6. Box plot of the pH in submicron aerosols calculated from the output of the AIM-II
721 model during the acidic particle periods in Pittsburgh during September 2002.

723
725
727
729
731
733
735
737
739
741
743
745
747
749
751
753



754 Figure S7. Comparisons of the mass spectra of hydrocarbon-like and oxygenated organic
755 aerosols determined independently for acidic and neutralized particle periods. c) and d) are the
756 same data plotted on logarithmic scale to better show the differences at high m/z 's.



815
816
817
818